

Orientable Hamilton Cycle Embeddings of Complete Tripartite Graphs II: Voltage Graph Constructions and Applications

M. N. Ellingham¹ and Justin Z. Schroeder²

¹DEPARTMENT OF MATHEMATICS, 1326 STEVENSON CENTER
VANDERBILT UNIVERSITY
NASHVILLE, TN 37240
E-mail: mark.ellingham@vanderbilt.edu

²DEPARTMENT OF MATHEMATICAL SCIENCES
GEORGE MASON UNIVERSITY
FAIRFAX, VA 22030
E-mail: jzschroeder@gmail.com

Received August 15, 2012; Revised December 5, 2013

Published online 21 January 2014 in Wiley Online Library (wileyonlinelibrary.com).
DOI 10.1002/jgt.21783

Abstract: In an earlier article the authors constructed a hamilton cycle embedding of $K_{n,n,n}$ in a nonorientable surface for all $n \geq 1$ and then used these embeddings to determine the genus of some large families of graphs. In this two-part series, we extend those results to orientable surfaces for all $n \neq 2$. In part II, a voltage graph construction is presented for building

Contract grant sponsor: National Security Agency; Contract grant number: H98230-09-1-0065. The United States Government is authorized to reproduce and distribute reprints notwithstanding any copyright notation herein.

Journal of Graph Theory
© 2014 Wiley Periodicals, Inc.

embeddings of the complete tripartite graph $K_{n,n,n}$ on an orientable surface such that the boundary of every face is a hamilton cycle. This construction works for all $n = 2p$ such that p is prime, completing the proof started by part I (which covers the case $n \neq 2p$) that there exists an orientable hamilton cycle embedding of $K_{n,n,n}$ for all $n \geq 1$, $n \neq 2$. These embeddings are then used to determine the genus of several families of graphs, notably $K_{t,n,n,n}$ for $t \geq 2n$ and, in some cases, $\overline{K_m} + K_n$ for $m \geq n - 1$. © 2014 Wiley Periodicals, Inc. J. Graph Theory 77: 219–236, 2014

Keywords: *complete tripartite graph; genus; graph embedding; hamilton cycle; voltage graph*

2000 Mathematics Subject Classification: *Primary 05C10*

1. INTRODUCTION

In [3], the present authors constructed nonorientable hamilton cycle embeddings of $K_{n,n,n}$ for all $n \geq 2$. In the first part of this series [4], we extended those results to the orientable case for all $n \geq 3$ such that $n \neq 2p$ for every prime p . In this article we complete the orientable case, constructing orientable hamilton cycle embeddings of $K_{n,n,n}$ for all $n = 2p$ where p is prime. To construct these embeddings, we present an embedded voltage graph whose derived embedding is the desired embedding of $K_{n,n,n}$. We use these embeddings, together with the embeddings found in [4], to determine the genus of several families of graphs, including $K_{t,n,n,n}$ for $t \geq 2n$ and, in certain cases, $\overline{K_m} + K_n$ for $m \geq n - 1$.

Earlier work on the genus of complete quadripartite graphs focused on the symmetric case of $K_{n,n,n,n}$. The orientable genus was determined by Jungerman [10], with White [19, p. 169] completing the case $n = 3$. Craft [2] later used different methods to verify the results for $n \neq 3, 5$. The nonorientable genus was also determined by Jungerman [11]. The genus of graphs in the family $\overline{K_m} + K_n$ has been investigated in a number of articles, including [2, 5, 9, 13, 15]. The work here extends that of the first author and Stephens in [6]. See [5, 6] for further references.

A basic understanding of topological graph theory is assumed. A *surface* is a compact 2-manifold without boundary. The orientable surface S_h is obtained by adding h handles to a sphere, and the *genus* of a graph G , denoted $g(G)$, is the minimum value of h for which G can be embedded on S_h . It is well known that a cellular embedding can be characterized, up to homeomorphism, by providing a set of facial walks that double cover the edges and yield a proper rotation at each vertex. To define a proper rotation, we must introduce the *rotation graph* at a vertex v , denoted R_v . If G is loopless, then R_v has as its vertex set the edges incident with v , and two edges u_1v and u_2v are joined by one edge for each occurrence of the subsequence $(\cdots u_1vu_2 \cdots)$, or its reverse, in one of the facial walks. R_v is 2-regular; we say it is *proper* if R_v consists of a single cycle. This ensures that the neighborhood around each vertex is homeomorphic to a disk. If G is a simple graph, we can think of R_v as a graph on the neighbors of v by identifying the edge uv with the vertex u ; in this article, we will use both interpretations of R_v . The embedding is orientable if and only if the faces can be oriented so that each edge appears once in each direction. For additional details and terminology, see [8]. For further background information on hamilton cycle embeddings, see [3].

We let $A = \{a_0, \dots, a_{n-1}\}$, $B = \{b_0, \dots, b_{n-1}\}$, and $C = \{c_0, \dots, c_{n-1}\}$ be the vertices of $K_{n,n,n}$ so that A , B , and C are the maximal independent sets. A hamilton cycle face of the form $(a_{j_0} b_{k_0} c_{\ell_0} a_{j_1} b_{k_1} c_{\ell_1} \dots a_{j_{n-1}} b_{k_{n-1}} c_{\ell_{n-1}})$ is called an *ABC cycle*; when this cycle is the boundary of a face we will refer to it as an *ABC face*. We call the edge $a_i b_j$ an *AB-edge of slope $j - i$* , and similarly for *BC edges* and *CA edges*.

2. PRELIMINARIES

We will use two main tools in this article. An embedded voltage graph is a common method used to build embeddings of highly symmetric graphs, while the diamond sum is a surgical technique that allows us to combine two known embeddings to get a new embedding.

A. Voltage Graphs

We assume the reader is familiar with voltage graphs and embedded voltage graphs; for a detailed explanation see [8]. We want to build an embedded voltage graph G_n with voltage assignment $\alpha : \vec{E}(G_n) \rightarrow \mathbb{Z}_n$ such that the derived embedded graph G_n^α is $K_{n,n,n}$. Here $\vec{E}(G_n)$ denotes the set of arcs, or directed edges, of G_n . To achieve this, we let $V(G_n) = \{a, b, c\}$ —one vertex corresponding to each of the independent sets A , B , and C —and let $\vec{E}(G_n)$ contain n arcs directed from a to b , n arcs from b to c , and n arcs from c to a . Each voltage from the abelian group \mathbb{Z}_n will be assigned to one of the arcs between each pair of vertices. If the arc e from a to b has voltage i , then e represents all *AB-edges of slope i* in $K_{n,n,n}$, and similarly for *BC* and *CA edges*. Since the vertices and arcs of our embedded voltage graph are known ahead of time, all we will need to do is specify the rotation around each vertex. It will suffice, then, to show that all of the faces in the derived embedding are hamilton cycles.

We will use i_v to denote the arc with voltage i that originates from vertex v , where $v \in \{a, b, c\}$. Additionally, we will use \bar{e} to denote that e is traced in the reverse direction. We do this to keep track of the directions in which each arc is traced, which will allow us to verify that the embeddings we construct are orientable. The following theorem and corollary will simplify the proofs in Section 3.

Theorem 2.1 (Gross and Tucker, Theorem 2.1.3 in [8]). *Let W be a closed walk of length k bounding a face in the embedded voltage graph $(G \rightarrow \Sigma, \alpha)$, and let the net voltage $|W|$ have order m in the voltage group Γ . Then W yields $\frac{|\Gamma|}{m}$ faces of size km in the derived embedding of G^α .*

Corollary 2.2. *Let $W_1 = (i_a j_b k_c)$ and $W_2 = (\bar{p}_c \bar{q}_b \bar{r}_a)$ be closed facial walks (described as a sequence of arcs) in an embedding of G_n as described above. If $\gcd(i + j + k, n) = 1$ (resp. $\gcd(-p - q - r, n) = 1$), then W_1 (resp. W_2) yields a single hamilton cycle face in the derived embedding.*

Proof. Theorem 2.1 implies that both W_1 and W_2 yield a single face of length $3n$ in the derived embedding. We must show that these faces are actually hamilton cycles. The resulting faces are shown below. For convenience, we set $\beta = i + j + k$ and $\gamma =$

$p + q + r$.

$W_1 : (a_0 \ b_i \ c_{i+j} \ a_\beta \ b_{i+\beta} \ c_{i+j+\beta} \ a_{2\beta} \ b_{i+2\beta} \ c_{i+j+2\beta} \dots a_{(n-1)\beta} \ b_{i+(n-1)\beta} \ c_{i+j+(n-1)\beta})$

$W_2 : (a_0 \ c_{-p} \ b_{-p-q} \ a_{-\gamma} \ c_{-p-\gamma} \ b_{-p-q-\gamma} \ a_{-2\gamma} \ c_{-p-2\gamma} \ b_{-p-q-2\gamma} \dots a_{-(n-1)\gamma} \ c_{-p-(n-1)\gamma} \ b_{-p-q-(n-1)\gamma})$

Because β and γ are both of order n in \mathbb{Z}_n , these are hamilton cycles. ■

B. Diamond Sum

The so-called “diamond sum” technique was introduced in dual form by Bouchet [1], reinterpreted by Magajna, Mohar, and Pisanski [14], developed further by Mohar, Parsons, and Pisanski [16], and generalized by Kawarabayashi, Stephens, and Zha [12]. In particular, the diamond sum construction allows us to combine embeddings of $K_{t_1, n, n, n}$ with genus g_1 and $K_{t_2, 3n}$ with genus g_2 to get an embedding of $K_{t_1+t_2-2, n, n, n}$ with genus $g_1 + g_2$. This is achieved by removing a disk containing a vertex of degree $3n$ and all of its incident edges from each embedding and identifying the boundaries of the resulting holes in a suitable fashion; we will do this in such a way that the final embedding is a genus embedding. For similar applications of the diamond sum, see [5–7], and for more information on this technique, see [17, pages 117–118].

3. VOLTAGE GRAPH CONSTRUCTIONS

We begin by presenting some special case constructions for $p = 2$ and $p = 3$.

Lemma 3.1. *For $p = 2$ or 3 , there exists an embedded voltage graph G_{2p} such that the derived embedding is an orientable hamilton cycle embedding of $K_{2p, 2p, 2p}$ with at least one ABC face.*

Proof. Let G_4 be the embedded voltage graph over \mathbb{Z}_4 given by the rotation scheme

$$\begin{aligned} R_a &: (0_a \ 1_a \ 2_a \ 3_a \ 0_c \ 3_c \ 2_c \ 1_c), \\ R_b &: (0_a \ 0_b \ 3_a \ 2_b \ 2_a \ 1_b \ 1_a \ 3_b), \\ R_c &: (0_c \ 0_b \ 1_c \ 1_b \ 2_c \ 3_b \ 3_c \ 2_b); \end{aligned}$$

and let G_6 be the embedded voltage graph over \mathbb{Z}_6 given by the rotation scheme

$$\begin{aligned} R_a &: (0_a \ 1_c \ 1_a \ 2_c \ 2_a \ 5_c \ 4_c \ 4_a \ 0_c \ 3_a \ 3_c \ 5_a), \\ R_b &: (0_a \ 2_b \ 1_a \ 3_b \ 4_a \ 5_b \ 3_a \ 4_b \ 2_a \ 1_b \ 5_a \ 0_b), \\ R_c &: (0_b \ 5_c \ 1_b \ 2_c \ 4_b \ 0_c \ 3_b \ 3_c \ 5_b \ 4_c \ 2_b \ 1_c). \end{aligned}$$

We leave it to the reader to verify that the given embeddings of G_4 and G_6 yield the required embeddings of $K_{4,4,4}$ and $K_{6,6,6}$, respectively. In each case, $(0_a 0_b 1_c)$ is a triangle face that yields an ABC face in the derived embedding via Corollary 2.2. ■

We are now going to give a general construction for $n = 2p$, where $p \geq 5$ is prime. The embedded voltage graph G_{2p} that we construct will consist of one $6p$ -gonal face Ω and $2p$ 3-faces $\Delta_0, \dots, \Delta_{p-1}, \Lambda_0, \dots, \Lambda_{p-1}$. To start out, we will present the closed walks we want to be facial boundaries in our embedded voltage graph by describing their sequence of arcs. Then, we will show that these walks yield hamilton cycles in the derived embedding. Finally, we will verify our embedded voltage graph is well-defined

by showing that the rotation graph around every vertex is proper. The voltage group we will be using for these graphs is $\mathbb{Z}_p \times \mathbb{Z}_2$; this group is isomorphic to \mathbb{Z}_{2p} but is preferred for notational convenience. For the remainder of this section, we simply write x for $(x, 0)$ and x^* for $(x, 1)$.

Definition 3.2. Let $p \geq 5$ be prime, and define the sequences $\omega_i = i_a (i+3)_b (p-2i-2)_c$ and $\theta_i = (p-2i)_c (i-1)_b \overline{i_a}$. Define Ω to be the closed walk given by the following sequence of arcs.

$$\Omega : \frac{(1_a^* (p-1)_b^* 0_c^* 0_a^* 3_b (p-2)_c \omega_1 \omega_2 \dots \omega_{p-3} \omega_{p-2}}{(p-1)_c^* 2_b^* (p-3)_a^* \theta_1 \theta_2 \dots \theta_{p-3} \theta_{p-2} \overline{2_c} (p-2)_b (p-1)_a^*)}$$

Lemma 3.3. For all prime $p \geq 5$, Ω yields $2p$ hamilton cycle faces in the derived embedding of $K_{2p,2p,2p}$.

Proof. It will suffice to show that one of the resulting faces in the derived embedding is a hamilton cycle. Starting with the vertex a_0 , we obtain the following facial boundary in the embedding of $K_{2p,2p,2p}$.

$$\begin{aligned} & (a_0 b_{1^*} c_0 a_{0^*} b_0 c_3 a_1 b_2 c_6 a_2 b_4 c_9 a_3 b_6 c_{12} \dots \\ & a_{(p-4)} b_{(p-8)} c_{(p-9)} a_{(p-3)} b_{(p-6)} c_{(p-6)} a_{(p-2)} b_{(p-4)} c_{(p-3)} \\ & a_{(p-1)} c_{0^*} b_{(p-2)} a_{1^*} c_{3^*} b_{3^*} a_{2^*} c_{6^*} b_{5^*} a_{3^*} c_{9^*} b_{7^*} \dots \\ & a_{(p-3)^*} c_{(p-9)^*} b_{(p-5)^*} a_{(p-2)^*} c_{(p-6)^*} b_{(p-3)^*} a_{(p-1)^*} c_{(p-3)^*} b_{(p-1)^*}) \end{aligned}$$

For the sake of clarity, we list the vertices below by the order in which they appear within each independent set. Note that the net voltages of ω_i and θ_i are both 1, the net voltages of the sequences $(i+3)_b (p-2i-2)_c (i+1)_a$ and $\overline{i_a} (p-2i-2)_c \overline{i_b}$ are both 2, and the net voltages of the sequences $(p-2i-2)_c (i+1)_a (i+4)_b$ and $(i-1)_b \overline{i_a} (p-2i-2)_c$ are both 3. This is evident in the following sequences.

$$\begin{aligned} A : & (a_0 a_{0^*} a_1 a_2 \dots a_{(p-2)} a_{(p-1)} a_{1^*} a_{2^*} \dots a_{(p-2)^*} a_{(p-1)^*}), \\ B : & (b_{1^*} b_0 b_2 b_4 \dots b_{(p-4)} b_{(p-2)} b_{3^*} b_{5^*} \dots b_{(p-3)^*} b_{(p-1)^*}), \\ C : & (c_0 c_3 c_6 c_9 \dots c_{(p-6)} c_{(p-3)} c_{0^*} c_{3^*} \dots c_{(p-6)^*} c_{(p-3)^*}). \end{aligned}$$

This cycle is clearly a hamilton cycle. Since Ω was a walk of length $6p$, it must be true that $|\Omega| = 0$. From Theorem 2.1, we know Ω yields $2p$ faces of length $6p$, each of which must be a hamilton cycle. ■

Before we provide the remaining faces, we want to construct the partial rotations at each vertex in the embedded voltage graph as determined by Ω . In the observation that follows, we use the notation $[a b c \dots d]$ to denote a path in the corresponding rotation (i.e., a is not adjacent to d in the rotation graph).

Lemma 3.4. The partial rotations determined by Ω consist of the following paths with the given endpoints. Each path is labeled for reference later in this section.

$$\begin{aligned} a : & P_1^A = [(p-3)_a^* \dots 1_a^*], P_3^A = [(p-1)_a^* 1_a^*], P_5^A = [0_c^* 0_a^*], \\ b : & P_1^B = [2_b \dots (p-1)_b], P_3^B = [2_b^* (p-3)_a^*], P_5^B = [0_a^* \dots (p-1)_a^*], \\ & P_7^B = [1_a^* (p-1)_b^*], \\ c : & P_1^C = [(p-1)_b \dots 2_b], P_3^C = [(p-1)_c^* 2_b^*], P_5^C = [(p-1)_b^* 0_c^*]. \end{aligned}$$

Proof. Let $\Omega_1 = (\omega_0 \omega_1 \dots \omega_{p-1})$ and $\Omega_2 = (\theta_0 \theta_1 \dots \theta_{p-1})$. The rotation around a determined by the closed walks Ω_1 and Ω_2 is given by

$$Q_1 = (0_a (p-2)_c 1_a (p-4)_c 2_a (p-6)_c \dots (p-2)_a 2_c (p-1)_a 0_c).$$

To construct Ω from Ω_1 and Ω_2 , we must first remove the subsequence $\omega_{p-1} \omega_0$ from Ω_1 and the subsequence $\theta_{p-1} \theta_0$ from Ω_2 . By doing so, we lose the subsequence $(p-2)_a 2_c (p-1)_a 0_c 0_a (p-2)_c 1_a$ from Q_1 , which results in a partial rotation around a given by

$$Q_2 = [1_a (p-4)_c 2_a (p-6)_c \dots (p-2)_a].$$

Finally, we add the sequences $\overline{\theta_{p-2} 2_c (p-2)_b (p-1)_a^* 1_a^* (p-1)_b^* 0_c^* 0_a^* 3_b (p-2)_c \omega_1}$ and $\overline{\omega_{p-2} (p-1)_c^* 2_b^* (p-3)_a^* \theta_1}$, which induce the following partial rotations around a .

$$P_1^A = [(p-3)_a^* (p-2)_c 1_a] Q_2 [(p-2)_a 2_c (p-1)_c^*],$$

$$P_3^A = [(p-1)_a^* 1_a], P_5^A = [0_c^* 0_a^*].$$

For the partial rotation around b determined by Ω , we again consider first the rotation around b determined by Ω_1 and Ω_2 , which is given by

$$R_1 = (0_a 3_b 4_a 7_b 8_a 11_b \dots (p-8)_a (p-5)_b (p-4)_a (p-1)_b).$$

Removing $\omega_{p-1} \omega_0$ and $\theta_{p-1} \theta_0$ results in a loss of the subsequences $(p-1)_b 0_a 3_b$ and $(p-2)_b (p-1)_a 2_b$ from R_1 ; this splits R_1 into the two partial rotations R_2 and R_3 shown below.

$$R_2 = [3_b 4_a 7_b 8_a 11_b \dots (p-2)_b],$$

$$R_3 = [2_b \dots (p-8)_a (p-5)_b (p-4)_a (p-1)_b].$$

Finally, we add in the remaining pieces of Ω to obtain the following partial rotations around b .

$$P_1^B = R_3, P_3^B = [2_b^* (p-3)_a^*], P_5^B = [0_a^* 3_b] R_2 [(p-2)_b (p-1)_a^*],$$

$$P_7^B = [1_a^* (p-1)_b^*].$$

Using a similar process on c , we get an initial rotation from Ω_1 and Ω_2 given by

$$S_1 = (0_c (p-1)_b 6_c (p-4)_b 12_c (p-7)_b \dots (p-12)_c 5_b (p-6)_c 2_b).$$

Removing $\omega_{p-1} \omega_0$ and $\theta_{p-1} \theta_0$ results in a loss of the subsequences $2_b 0_c (p-1)_b$, $3_b (p-2)_c$ and $2_c (p-2)_b$ from S_1 ; this splits S_1 into three partial rotations. Note, however, that the subsequences $3_b (p-2)_c$ and $2_c (p-2)_b$ are included in the remaining pieces of Ω , so the removal of the subsequence $2_b 0_c (p-1)_b$ yields a partial rotation around c given by

$$S_2 = [(p-1)_b 6_c (p-4)_b 12_c (p-7)_b \dots (p-12)_c 5_b (p-6)_c 2_b].$$

Adding in the unused subsequences from Ω results in the following partial rotations around c .

$$P_1^C = S_2, P_3^C = [(p-1)_c^* 2_b^*], P_5^C = [(p-1)_b^* 0_c^*].$$

■

We now progress to the $2p$ 3-cycles that will complete our embedded voltage graph. Because we want to use each arc once as e and once as \bar{e} , we define p 3-cycles with arc

TABLE I. Required 3-cycles of the form $\Delta = (i_a j_b k_c)$, where $h = \frac{p-1}{2}$.

Cycle $(i_a j_b k_c)$	i	j	k	Net Voltage
Δ_0	0	2^*	0	2^*
Δ_1	3^*	1^*	$(p-3)^*$	1^*
\vdots	\vdots	\vdots	\vdots	\vdots
Δ_ℓ	$(2\ell+1)^*$	$(2\ell-1)^*$	$(p-2\ell-1)^*$	$(2\ell-1)^*$
\vdots	\vdots	\vdots	\vdots	\vdots
Δ_{h-1}	$(p-2)^*$	$(p-4)^*$	2^*	$(p-4)^*$
Δ_h	$p-1$	2	3^*	4^*
Δ_{h+1}	2^*	4^*	$(p-2)^*$	4^*
\vdots	\vdots	\vdots	\vdots	\vdots
Δ_ℓ	$(2\ell+1)^*$	$(2\ell+3)^*$	$(p-2\ell-1)^*$	$(2\ell+3)^*$
\vdots	\vdots	\vdots	\vdots	\vdots
Δ_{p-3}	$(p-5)^*$	$(p-3)^*$	5^*	$(p-3)^*$
Δ_{p-2}	$(p-3)^*$	$(p-2)^*$	1^*	$(p-4)^*$
Δ_{p-1}	$(p-1)^*$	0^*	$(p-1)^*$	$(p-2)^*$

TABLE II. Required 3-cycles of the form $\Lambda = (\bar{i}_c \bar{j}_b \bar{k}_a)$, where $h = \frac{p-1}{2}$.

Cycle $(\bar{i}_c \bar{j}_b \bar{k}_a)$	i	j	k	Net Voltage
Λ_0	0	$(p-1)^*$	$p-1$	2^*
Λ_1	1^*	$(p-3)^*$	0^*	2^*
Λ_2	3^*	$(p-5)^*$	$(p-5)^*$	7^*
\vdots	\vdots	\vdots	\vdots	\vdots
Λ_ℓ	$(2\ell-1)^*$	$(p-2\ell-1)^*$	$(p-2\ell-1)^*$	$(2\ell+3)^*$
\vdots	\vdots	\vdots	\vdots	\vdots
Λ_{h-2}	$(p-6)^*$	4^*	4^*	$(p-2)^*$
Λ_{h-1}	$(p-4)^*$	$(p-4)^*$	2^*	6^*
Λ_h	$(p-2)^*$	$(p-6)^*$	$(p-2)^*$	10^*
Λ_{h+1}	0^*	$p-1$	0	1^*
Λ_{h+2}	2^*	$(p-8)^*$	$(p-4)^*$	10^*
\vdots	\vdots	\vdots	\vdots	\vdots
Λ_ℓ	$(2\ell-1)^*$	$(p-2\ell-5)^*$	$(p-2\ell-1)^*$	$(2\ell+7)^*$
\vdots	\vdots	\vdots	\vdots	\vdots
Λ_{p-3}	$(p-7)^*$	1^*	5^*	1^*
Λ_{p-2}	$(p-5)^*$	$(p-2)^*$	3^*	4^*
Λ_{p-1}	$(p-3)^*$	0^*	1^*	2^*

sequences of the form $(i_a j_b k_c)$ and the other p 3-cycles with arc sequences of the form $(\bar{i}_c \bar{j}_b \bar{k}_a)$. Cycles of the first form are presented in Table I, while cycles of the second form are presented in Table II. In both tables, we let $h = \frac{p-1}{2}$.

Before the main theorem is proved, we again make an observation about the partial rotations determined by the Δ_i 's and Λ_i 's.

Lemma 3.5. *Let $p \geq 11$. The partial rotations determined by the Δ_i 's and Λ_j 's consist of the following paths with the given endpoints. Each path is again labeled for future reference.*

$$\begin{aligned} a : P_2^A &= [(p-1)_c^* (p-1)_a^*], P_4^A = [1_a^* \dots 0_c^*], P_6^A = [0_a^* 1_c^* (p-3)_a^*], \\ b : P_2^B &= [(p-1)_b 0_a 2_b^*], P_4^B = [(p-3)_a^* \dots 0_a^*], P_6^B = [(p-1)_a^* 0_b^* 1_a^*], \\ P_8^B &= [(p-1)_b^* (p-1)_a 2_b], \\ c : P_2^C &= [2_b \dots (p-1)_c^*], P_4^C = [2_b^* 0_c (p-1)_b^*], P_6^C = [0_c^* (p-1)_b]. \end{aligned}$$

Proof. For the rotation around a , observe that the families $\{\Delta_\ell \mid 1 \leq \ell \leq h-1\}$ and $\{\Lambda_\ell \mid h+2 \leq \ell \leq p-3\}$ yield the partial rotations

$$\begin{aligned} Q_1 &= [(p-5)_c^* 5_a^* (p-7)_c^* 7_a^* (p-9)_c^* 9_a^* \dots 4_c^* (p-4)_a^* 2_c^* (p-2)_a^*], \\ Q_2 &= [(p-3)_c^* 3_a^*], \end{aligned}$$

and the families $\{\Delta_\ell \mid h+1 \leq \ell \leq p-3\}$ and $\{\Lambda_\ell \mid 2 \leq \ell \leq h-2\}$ yield the partial rotations

$$\begin{aligned} Q_3 &= [(p-4)_c^* 4_a^* (p-6)_c^* 6_a^* (p-8)_c^* 8_a^* \dots (p-7)_a^* 5_c^* (p-5)_a^* 3_c^*], \\ Q_4 &= [(p-2)_c^* 2_a^*]. \end{aligned}$$

By considering the remaining 3-cycles—namely $\Delta_0, \Delta_h, \Delta_{p-2}, \Delta_{p-1}, \Lambda_0, \Lambda_1, \Lambda_{h-1}, \Lambda_h, \Lambda_{h+1}, \Lambda_{p-2}$ and Λ_{p-1} , where $h = \frac{p-1}{2}$ —we learn that the partial rotations around a are the following.

$$\begin{aligned} P_2^A &= [(p-1)_c^* (p-1)_a^*], \\ P_4^A &= [1_a^* (p-3)_c^*] Q_2 [3_a^* (p-5)_c^*] Q_1 [(p-2)_a^* (p-2)_c^*] Q_4 [2_a^* (p-4)_c^*] \\ &\quad Q_3 [3_c^* (p-1)_a 0_c 0_a 0_c^*], \\ P_6^A &= [0_a^* 1_c^* (p-3)_a^*]. \end{aligned}$$

For the rotation around b , observe that the families $\{\Delta_\ell \mid 1 \leq \ell \leq h-1\}$ and $\{\Lambda_\ell \mid h+2 \leq \ell \leq p-3\}$ yield the partial rotations

$$\begin{aligned} R_1 &= [3_a^* 1_b^* 5_a^* 3_b^* 7_a^* 5_b^* \dots (p-6)_a^* (p-8)_b^* (p-4)_a^* (p-6)_b^*], \\ R_2 &= [(p-2)_a^* (p-4)_b^*]. \end{aligned}$$

and the families $\{\Delta_\ell \mid h+1 \leq \ell \leq p-3\}$ and $\{\Lambda_\ell \mid 2 \leq \ell \leq h-2\}$ yield the partial rotation

$$R_3 = [2_a^* 4_b^* 4_a^* 6_b^* 6_a^* 8_b^* \dots (p-7)_a^* (p-5)_b^* (p-5)_a^* (p-3)_b^*].$$

By considering the remaining Δ and Λ cycles, we learn that the partial rotations around b are the following.

$$\begin{aligned} P_2^B &= [(p-1)_b 0_a 2_b^*], \\ P_4^B &= [(p-3)_a^* (p-2)_b^* 3_a^*] R_1 [(p-6)_b^* (p-2)_a^*] R_2 [(p-4)_b^* 2_a^*] R_3 [(p-3)_b^* 0_a^*], \\ P_6^B &= [(p-1)_a^* 0_b^* 1_a^*], \\ P_8^B &= [(p-1)_b^* (p-1)_a 2_b]. \end{aligned}$$

For the rotation around c , we consider two cases. If $p \equiv 1 \pmod{4}$, then h is even. Observe that the families $\{\Delta_\ell \mid 1 \leq \ell \leq h-1\}$ and $\{\Lambda_\ell \mid h+2 \leq \ell \leq p-3\}$ yield the

partial rotations

$$S_1 = [(p-4)_b^* 2_c^* (p-8)_b^* 6_c^* (p-12)_b^* 10_c^* \dots 5_b^* (p-7)_c^* 1_b^* (p-3)_c^*],$$

$$S_2 = [(p-6)_b^* 4_c^* (p-10)_b^* 8_c^* (p-14)_b^* 12_c^* \dots 7_b^* (p-9)_c^* 3_b^* (p-5)_c^*],$$

and the families $\{\Delta_\ell \mid h+1 \leq \ell \leq p-3\}$ and $\{\Lambda_\ell \mid 2 \leq \ell \leq h-2\}$ yield the partial rotations

$$S_3 = [(p-3)_b^* 5_c^* (p-7)_b^* 9_c^* (p-11)_b^* 13_c^* \dots 10_b^* (p-8)_c^* 6_b^* (p-4)_c^*],$$

$$S_4 = [3_c^* (p-5)_b^* 7_c^* (p-9)_b^* 11_c^* (p-13)_b^* \dots 8_b^* (p-6)_c^* 4_b^* (p-2)_c^*].$$

By considering the remaining Δ and Λ cycles, we learn that the partial rotations around c are the following.

$$P_2^C = [2_b^* 3_c^*] S_4 [(p-2)_c^* (p-6)_b^*] S_2 [(p-5)_c^* (p-2)_b^* 1_c^* (p-3)_b^*] S_3$$

$$[(p-4)_c^* (p-4)_b^*] S_1 [(p-3)_c^* 0_b^* (p-1)_c^*],$$

$$P_4^C = [2_b^* 0_c^* (p-1)_b^*],$$

$$P_6^C = [0_c^* (p-1)_b^*].$$

On the other hand, if $p \equiv 3 \pmod{4}$, then h is odd. Observe that the families $\{\Delta_\ell \mid 1 \leq \ell \leq h-1\}$ and $\{\Lambda_\ell \mid h+2 \leq \ell \leq p-3\}$ yield the partial rotations

$$S_1 = [(p-4)_b^* 2_c^* (p-8)_b^* 6_c^* (p-12)_b^* 10_c^* \dots 7_b^* (p-9)_c^* 3_b^* (p-5)_c^*],$$

$$S_2 = [(p-6)_b^* 4_c^* (p-10)_b^* 8_c^* (p-14)_b^* 12_c^* \dots 5_b^* (p-7)_c^* 1_b^* (p-3)_c^*],$$

and the families $\{\Delta_\ell \mid h+1 \leq \ell \leq p-3\}$ and $\{\Lambda_\ell \mid 2 \leq \ell \leq h-2\}$ yield the partial rotations

$$S_3 = [(p-3)_b^* 5_c^* (p-7)_b^* 9_c^* (p-11)_b^* 13_c^* \dots 8_b^* (p-6)_c^* 4_b^* (p-2)_c^*],$$

$$S_4 = [3_c^* (p-5)_b^* 7_c^* (p-9)_b^* 11_c^* (p-13)_b^* \dots 10_b^* (p-8)_c^* 6_b^* (p-4)_c^*].$$

By considering the remaining Δ and Λ cycles, we learn that the partial rotations around c are the following.

$$P_2^C = [2_b^* 3_c^*] S_4 [(p-4)_c^* (p-4)_b^*] S_1 [(p-5)_c^* (p-2)_b^* 1_c^* (p-3)_b^*] S_3$$

$$[(p-2)_c^* (p-6)_b^*] S_2 [(p-3)_c^* 0_b^* (p-1)_c^*],$$

$$P_4^C = [2_b^* 0_c^* (p-1)_b^*],$$

$$P_6^C = [0_c^* (p-1)_b^*].$$

■

By concatenating the paths representing the partial rotations given by Lemmas 3.4 and 3.5, we get the following cycles which, as we will see later, represent the complete rotation graphs around the vertices a , b , and c .

Lemma 3.6. *Let $p \geq 5$ be prime. The following are cycles of length $4p$.*

$$R_a : (P_1^A P_2^A P_3^A P_4^A P_5^A P_6^A),$$

$$R_b : (P_1^B P_2^B P_3^B P_4^B P_5^B P_6^B P_7^B P_8^B),$$

$$R_c : (P_1^C P_2^C P_3^C P_4^C P_5^C P_6^C).$$

Proof. By concatenating the corresponding paths, it is clear that R_a is a closed walk. Moreover, each of the $2p$ arcs from a to b and each of the $2p$ arcs from c to a appears either exactly once in the interior of one of the partial rotation paths, or appears as the

endpoint of two different partial rotation paths. Therefore each arc appears exactly once in R_a , so R_a is a cycle of length $4p$. Similar arguments apply for both R_b and R_c . ■

We are now able to construct hamilton cycle embeddings of $K_{n,n,n}$ whenever $n = 2p$ for a prime p .

Theorem 3.7. *Let $p \geq 11$ be prime. The embedding given by the faces $\Omega, \Delta_0, \dots, \Delta_{p-1}, \Lambda_0, \dots, \Lambda_{p-1}$ is an embedded voltage graph G_{2p} whose derived embedding is an orientable hamilton cycle embedding of $K_{2p,2p,2p}$ with at least one ABC face.*

Proof. From the way the faces $\Omega, \Delta_0, \dots, \Delta_{p-1}, \Lambda_0, \dots, \Lambda_{p-1}$ were constructed, we know each arc is used once as e and once as \bar{e} ; thus, the embedding given by these faces is orientable. Moreover, the rotation graphs that we obtain from these faces are given by Lemma 3.6. Since R_a, R_b , and R_c consist of a single cycle, our voltage graph G_{2p} is embedded in some orientable surface. It follows that the derived embedding is an orientable embedding of $K_{2p,2p,2p}$; thus, it remains to show that the boundary of every face is a hamilton cycle. From Lemma 3.3 we know Ω yields $2p$ hamilton cycles in the derived embedding. To show that all of the 3-cycles yield hamilton cycles, we use the isomorphism from $\mathbb{Z}_p \times \mathbb{Z}_2$ to \mathbb{Z}_{2p} induced by mapping the generator 1^* to 1. Under this mapping, Corollary 2.2 implies that it suffices to show $|\Delta_i|$ and $|\Lambda_i|$ are of order $2p$ in the group $\mathbb{Z}_p \times \mathbb{Z}_2$. This is true as long as $|\Delta_i| = x^*$ and $|\Lambda_i| = y^*$ for some $x, y \in \mathbb{Z}_p \setminus \{0\}$. From Tables I and II this condition is satisfied, so all of the 3-cycles yield hamilton cycles as well. Thus, the derived embedding from the embedded voltage graph given by $\Omega, \Delta_0, \dots, \Delta_{p-1}, \Lambda_0, \dots, \Lambda_{p-1}$ is a hamilton cycle embedding of $K_{2p,2p,2p}$. Observe that the faces derived from the Δ_i 's and Λ_i 's are all ABC faces. ■

The following lemma covers the remaining cases $p = 5$ and $p = 7$ by making a slight modification to the construction above.

Lemma 3.8. *For $p = 5$ or 7 , there exists an embedded voltage graph such that the derived embedding is an orientable hamilton cycle embedding of $K_{2p,2p,2p}$ with at least one ABC face.*

Proof. The construction uses Ω together with the 3-cycles shown in Table III. The resulting rotations for $p = 5$ are

$$\begin{aligned} a &: (0_a 0_c^* 0_a^* 1_c^* 2_a^* 3_c 1_a 1_c 2_a 4_c 3_a 2_c 4_c^* 4_a^* 1_a^* 2_c^* 3_a^* 3_c^* 4_a 0_c), \\ b &: (0_b 1_a 4_b 0_a 2_b^* 2_a^* 3_b^* 3_a^* 1_b^* 0_a^* 3_b 4_a^* 0_b^* 1_a^* 4_b^* 4_a 2_b 3_a 1_b 2_a), \\ c &: (0_c 4_b^* 0_c^* 4_b 1_c 1_b 2_c 3_b 3_c 0_b 4_c 2_b 3_c^* 3_b^* 1_c^* 1_b^* 2_c^* 0_b^* 4_c^* 2_b^*), \end{aligned}$$

and for $p = 7$ are

$$\begin{aligned} a &: (0_a 0_c^* 0_a^* 1_c^* 4_a^* 5_c 1_a 3_c 2_a 1_c 3_a 6_c 4_a 4_c 5_a 2_c 6_c^* 6_a^* 1_a^* 4_c^* 3_a^* 2_c^* 5_a^* 5_c^* 2_a^* 3_c^* 6_a 0_c), \\ b &: (0_b 1_a 4_b 5_a 1_b 2_a 5_b 6_a^* 0_b^* 1_a^* 6_b^* 6_a 2_b 3_a 6_b 0_a 2_b^* 4_a^* 5_b^* 3_a^* 1_b^* 5_a^* 3_b^* 2_a^* 4_b^* 0_a^* 3_b 4_a), \\ c &: (0_c 6_b^* 0_c^* 6_b 6_c 3_b 5_c 0_b 4_c 4_b 3_c 1_b 2_c 5_b 1_c 2_b 3_c^* 3_b^* 2_c^* 5_b^* 1_c^* 4_b^* 5_c^* 1_b^* 4_c^* 0_b^* 6_c^* 2_b^*). \end{aligned} \quad \blacksquare$$

4. SUMMARY OF ORIENTABLE HAMILTON CYCLE EMBEDDINGS OF $K_{n,n,n}$

We first recall the following theorem from [4].

TABLE III. Required 3-cycles for $p = 5$ and 7.

	Cycle $(i_a j_b k_c)$	i	j	k	Net Voltage	Cycle $(\overline{i_c} \overline{j_b} \overline{k_a})$	i	j	k	Net Voltage
$p = 5$	Δ_0	0	2*	0	2*	Δ_0	0	4*	4	3*
	Δ_1	3*	1*	2*	1*	Δ_1	1*	1*	0*	2*
	Δ_2	4	2	3*	4*	Δ_2	3*	3*	3*	4*
	Δ_3	2*	3*	1*	1*	Δ_3	0*	4	0	4*
	Δ_4	4*	0*	4*	3*	Δ_4	2*	0*	1*	3*
$p = 7$	Δ_0	0	2*	0	2*	Δ_0	0	6*	6	5*
	Δ_1	3*	1*	4*	1*	Δ_1	1*	4*	0*	5*
	Δ_2	5*	3*	2*	3*	Δ_2	3*	3*	2*	1*
	Δ_3	6	2	3*	4*	Δ_3	5*	1*	5*	4*
	Δ_4	2*	4*	5*	4*	Δ_4	0*	6	0	6*
	Δ_5	4*	5*	1*	3*	Δ_5	2*	5*	3*	3*
	Δ_6	6*	0*	6*	5*	Δ_6	4*	0*	1*	5*

Theorem 4.1 (Theorem 9.1 of [4]). *If $n \geq 1$ such that $n \neq 2$ and $n \neq 2p$ for every prime p , then there exists an orientable face 2-colorable hamilton cycle embedding of $K_{n,n,n}$ in which every face is an ABC face.*

Combining this result with the voltage graph construction, we can prove a complete result for orientable hamilton cycle embeddings of $K_{n,n,n}$.

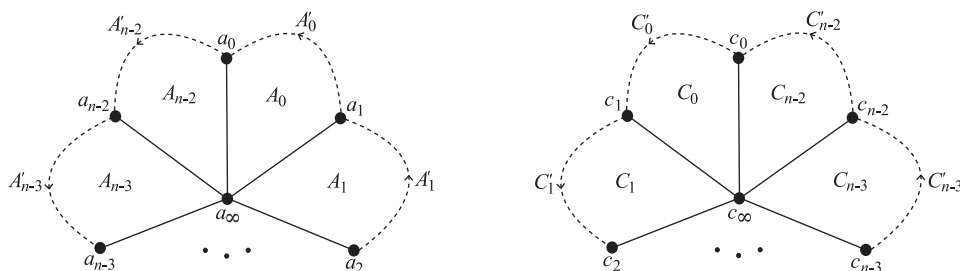
Theorem 4.2. *There exists an orientable hamilton cycle embedding of $K_{n,n,n}$ for all $n \geq 1$, $n \neq 2$, with at least one ABC face. There is no orientable hamilton cycle embedding of $K_{2,2,2}$.*

Proof. If $n \geq 1$ such that $n \neq 2$ and $n \neq 2p$ for every prime p , then the desired embedding is given by Theorem 4.1. If $n = 4$ or 6, then the desired embedding is given by Lemma 3.1. If $n = 10$ or 14, the desired embedding is given by Lemma 3.8. Finally, if $n = 2p$ for a prime $p \geq 11$, the desired embedding is given by Theorem 3.7.

Suppose we have a hamilton cycle embedding of $K_{2,2,2}$. The rotation graph at a_0 is a 4-cycle where b_0 and b_1 are either adjacent or not. If they are adjacent, we can assume without loss of generality that $R_{a_0} = (b_0 b_1 c_0 c_1)$, which provides the partial facial boundaries $(\dots b_0 a_0 b_1 \dots)$, $(\dots b_1 a_0 c_0 \dots)$, $(\dots c_0 a_0 c_1 \dots)$ and $(\dots c_1 a_0 b_0 \dots)$. A simple exhaustive search shows that there are three ways to complete these facial boundaries so all the rotation graphs are proper, and each of these results in a nonorientable embedding. If b_0 and b_1 are not adjacent, a similar analysis assuming a rotation graph of $(b_0 c_0 b_1 c_1)$ at a_0 yields seven hamilton cycle embeddings, all of which are nonorientable. (The full analysis can be done by hand, although this is somewhat lengthy and tedious; it is quickly accomplished by a simple computer program.) ■

5. GENUS OF SOME JOINS OF EDGELESS GRAPHS WITH COMPLETE GRAPHS

This section is an extension of the work of Ellingham and Stephens in [6]. We start by presenting two useful lemmas; we note here that Lemma 5.2 was proved using the diamond sum technique described briefly in Section 2.

FIGURE 1. Rotations and faces for hamilton cycle embedding of K_n .

Lemma 5.1 (Lemma 4.1 in [6]). *Let G be an m -regular simple graph on n vertices, with $m \geq 2$. The following are equivalent.*

- (i) G has an orientable hamilton cycle embedding.
- (ii) $\overline{K_m} + G$ has an orientable triangulation.
- (iii) $g(\overline{K_m} + G) = g(K_{m,n})$ and $4 \mid (m-2)(n-2)$.

Lemma 5.2 (Lemma 2.2 in [6]). *Let $n \geq 1$ and $m \geq n-1$ be integers. If $g(\overline{K_m} + K_n) = g(K_{m,n})$ and $4 \mid (m-2)(n-2)$, then $g(\overline{K_{m'}} + K_n) = g(K_{m',n})$ for all $m' \geq m$.*

Using the first lemma, we can determine the genus of $\overline{K_{n-1}} + K_n$ from orientable hamilton cycle embeddings of K_n . Using the second lemma, we can extend this result to $\overline{K_m} + K_n$ for all $m \geq n-1$. To that end, we present a recursive construction for orientable hamilton cycle embeddings of complete graphs. Our construction is a slight extension of the following result.

Theorem 5.3 (Theorem 4.3 in [6]). *Suppose $n \equiv 2 \pmod{4}$ and $n \geq 6$. If K_n has an orientable hamilton cycle embedding, then K_{2n-2} also has an orientable hamilton cycle embedding.*

Instead of a recursive construction that roughly doubles the number of vertices, we will roughly triple it.

Theorem 5.4. *Suppose $n \geq 4$ and K_n has an orientable hamilton cycle embedding. Then K_{3n-3} also has an orientable hamilton cycle embedding.*

Proof. Suppose K_n has an orientable hamilton cycle embedding, and provide each vertex with a clockwise rotation. This induces a counterclockwise direction on the boundary of each face.

Take one copy of the embedding, which we will denote by G_a , and label any vertex a_{∞} . Label the remaining vertices a_0, a_1, \dots, a_{n-2} in clockwise order as they appear in the rotation around a_{∞} . For each $i \in \mathbb{Z}_{n-1}$, let A_i denote the face that follows the path $a_i a_{\infty} a_{i+1}$ as it passes through a_{∞} . Let $G'_a = G_a - a_{\infty}$ be the graph on vertex set $V_a = \{a_i \mid i \in \mathbb{Z}_{n-1}\}$ obtained by removing a_{∞} and all of its incident edges from G_a . Each face A_i now becomes a directed path $A'_i = A_i - a_{\infty}$ from a_{i+1} to a_i in G'_a . This rotation scheme and the resulting paths can be seen in Figure 1. We take another copy of the embedding of K_n and construct the graph G'_b on vertex set $V_b = \{b_i \mid i \in \mathbb{Z}_{n-1}\}$ in an identical manner, replacing each a_i and A'_i with b_i and B'_i , respectively. We take a third copy of the embedding of K_n and construct the graph G'_c on vertex set $V_c = \{c_i \mid i \in \mathbb{Z}_{n-1}\}$

in a similar manner, only the vertices are labeled $c_0, c_{n-2}, c_{n-3}, \dots, c_2, c_1$ in clockwise order as they appear in the rotation around c_∞ . The resulting C'_i is now a directed path from c_i to c_{i+1} . This rotation scheme and the resulting paths can also be seen in Figure 1.

Let F_∞ be the directed cycle $(c_{n-2}b_{n-2}a_{n-2}c_{n-3}b_{n-3}a_{n-3} \dots c_1b_1a_1c_0b_0a_0)$, and let $\overline{F_\infty}$ be the underlying undirected cycle. For each $i \in \mathbb{Z}_{n-1}$, let F_i be the directed cycle $A'_i \cup B'_{i-1} \cup C'_{i-1} \cup \{a_ib_i, b_{i-1}c_{i-1}, c_ia_{i+1}\}$. These new directed edges a_ib_i , $b_{i-1}c_{i-1}$ and c_ia_{i+1} are the reverse of edges in F_∞ . Therefore, the collection $\mathcal{F} = \{F_i \mid i \in \mathbb{Z}_{n-1}\} \cup \{F_\infty\}$ covers every edge of the graph $H_1 = G'_a \cup G'_b \cup G'_c \cup \overline{F_\infty}$ (on vertex set $V_a \cup V_b \cup V_c$) once in each direction. It is clear from construction that every face is actually a hamilton cycle in H_1 ; we claim the collection \mathcal{F} determines an orientable hamilton cycle embedding of H_1 . To do so, it suffices to show that the rotation around each vertex is a single cycle. We will prove this for an arbitrary vertex a_i . Assume the rotation around a_i in G_a is given by the cycle $(a_\infty a_{\pi(1)} a_{\pi(2)} \dots a_{\pi(n-2)})$. This rotation stays the same except for the subsequence $(\dots a_{\pi(n-2)} a_\infty a_{\pi(1)} \dots)$. Instead of the paths $a_{\pi(n-2)} a_i a_\infty$ and $a_\infty a_i a_{\pi(1)}$ appearing in the cycles A_i and A_{i-1} , respectively, we have the paths $a_{\pi(n-2)} a_i b_i$ in F_i , $b_i a_i c_{i-1}$ in F_∞ , and $c_{i-1} a_i a_{\pi(1)}$ in F_{i-1} . Thus, the rotation around a_i in H_1 is given by $(b_i c_{i-1} a_{\pi(1)} a_{\pi(2)} \dots a_{\pi(n-2)})$, which is a single cycle. An analogous argument works for the rotations around b_i and c_i , so our claim is correct.

By Theorem 4.2, there exists a hamilton cycle embedding of $H_2 = K_{n-1, n-1, n-1}$ with at least one ABC face, call it D . We can label the vertices of H_2 so that D is the reverse of F_∞ ; this forces V_a , V_b , and V_c to be the tripartition of H_2 .

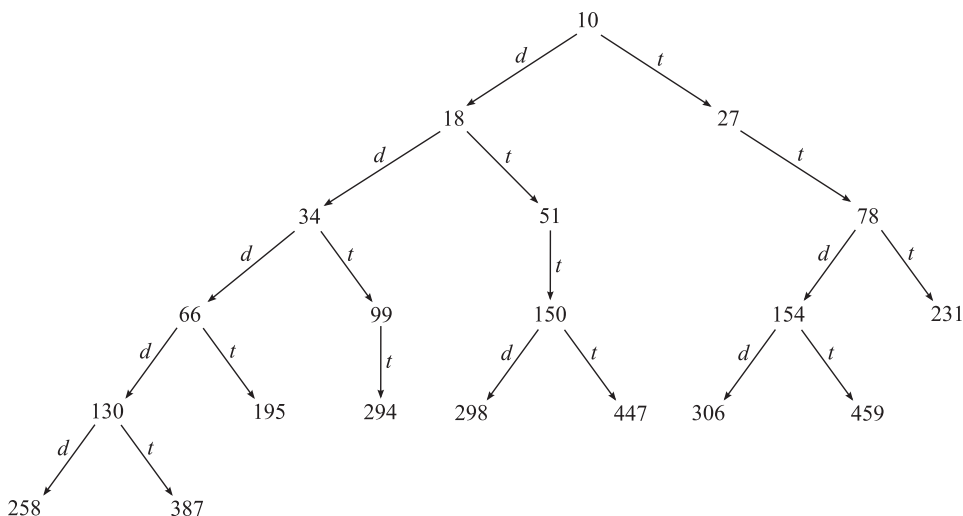
Delete the interior of the face F_∞ in H_1 to get an embedding with boundary curve $\overline{F_\infty}$. Also delete the interior of the face D in H_2 to get another embedding with boundary curve $\overline{F_\infty}$. The two embeddings share no edges except those in $\overline{F_\infty}$, so we can glue them together by identifying their boundary curves. The result is an orientable embedding of $H_1 \cup H_2$ such that every face is a hamilton cycle on $V_a \cup V_b \cup V_c$. Since G_a , G_b , and G_c are complete graphs on V_a , V_b , and V_c , respectively, and H_2 is the complete tripartite graph with independent sets V_a , V_b , and V_c , $H_1 \cup H_2$ is simply the complete graph on vertex set $V_a \cup V_b \cup V_c$. Therefore, we have an orientable hamilton cycle embedding of K_{3n-3} . ■

Starting with a known orientable hamilton cycle embedding of K_n , we can apply both the doubling construction (if $n \equiv 2 \pmod{4}$) and tripling construction (if $n \equiv 2$ or $3 \pmod{4}$) to obtain a family of embeddings of complete graphs. By Lemmas 5.1 and 5.2, having an orientable hamilton cycle embedding of K_n is equivalent to having a genus embedding of $\overline{K_m} + K_n$ for all $m \geq n-1$. Note that the condition $m \geq n-1$ allows us to view the embedding of $\overline{K_m} + K_n$ as an embedding of $K_{m,n}$ with some edges added to form a complete graph on the partite set of size n . Repeated application of the doubling construction to an embedding of K_{10} led to the following result.

Theorem 5.5 (Theorem 4.4 in [6]). *If $n = 2^p + 2$ for some $p \geq 3$, then $g(\overline{K_m} + K_n) = \lceil \frac{(m-2)(n-2)}{4} \rceil$ for all $m \geq n-1$.*

Now, if we take the underlying embeddings of K_n from Theorem 5.5 and repeatedly apply the tripling construction, we obtain the following result. In the case when q is odd, this theorem presents the first infinite family of values of n congruent to 3 modulo 4 for which the genus of $\overline{K_m} + K_n$ is known for all $m \geq n-1$.

Theorem 5.6. *If $n = 3^q(2^p + \frac{1}{2}) + \frac{3}{2}$ for some $p \geq 3$ and $q \geq 0$, then $g(\overline{K_m} + K_n) = g(K_{m,n}) = \lceil \frac{(m-2)(n-2)}{4} \rceil$ for all $m \geq n-1$.*

FIGURE 2. A tree showing $m \in T(10)$ with $m \leq 500$.

Proof. If $q = 0$, then this is equivalent to Theorem 5.5. For $q \geq 1$ and a fixed p , take the orientable hamilton cycle embedding of K_{2^p+2} generated by Theorem 5.5 and Lemma 5.1; the result is obtained by induction on q using Theorem 5.4 together with Lemmas 5.1 and 5.2. ■

This easily extends to the following result.

Corollary 5.7. Let $n = 3^q(2^p + \frac{1}{2}) + \frac{3}{2}$ for some $p \geq 3$ and $q \geq 0$. If G is any n -vertex simple graph, then $g(\overline{K_m} + G) = g(K_{m,n}) = \lceil \frac{(m-2)(n-2)}{4} \rceil$ for all $m \geq n - 1$.

We can further extend these results using the following lemma.

Lemma 5.8 (Lemma 2.4 in [6]). If $g(\overline{K_m} + K_n) = g(K_{m,n})$ for all $m \geq n - 1$, then $g(\overline{K_{m'}} + K_{n-1}) = g(K_{m',n-1})$ for all $m' \geq n$.

Corollary 5.9. Let $n = 3^q(2^p + \frac{1}{2}) + \frac{1}{2}$ for some $p \geq 3$ and $q \geq 0$. If G is any n -vertex simple graph, then $g(\overline{K_m} + G) = g(K_{m,n}) = \lceil \frac{(m-2)(n-2)}{4} \rceil$ for all $m \geq n + 1$.

So far, we have only used repeated applications of the doubling construction followed by repeated applications of the tripling construction; however, we can mix and match these constructions in any order, so long as the congruence condition modulo 4 is satisfied. From any value n for which an orientable hamilton cycle embedding of K_n is known to exist, we can construct an infinite set of values $T(n)$ such that an orientable hamilton cycle embedding of K_m exists for all $m \in T(n)$. The set is constructed recursively as follows: for any value $m \in T(n)$, if $m \equiv 2 \pmod{4}$, then $2m - 2$ and $3m - 3$ are also in $T(n)$ by virtue of the doubling construction given in [6] and the tripling construction given by Theorem 5.4, respectively; if $m \equiv 3 \pmod{4}$, then only $3m - 3$ is also in $T(n)$. A tree depicting the first 20 values in $T(10)$ and how they were obtained is shown in Figure 2. An edge labeled by d represents a link formed by virtue of the doubling construction, while an edge labeled by t represents a link formed by virtue of the tripling construction.

All of the results in Theorems 5.5 and 5.6 and Corollaries 5.7 and 5.9 were obtained by repeated applications of the doubling and tripling constructions to an orientable hamilton cycle embedding of K_{10} . If we were to find more families of embeddings to serve as building blocks, this would greatly enhance the power of these constructions. While preparing the final revision of this article we were given details of an unpublished construction by Jozef Širáň for an orientable hamilton cycle embedding of K_{15} , which involves gluing together three embeddings derived from embedded voltage graphs. $T(15)$ covers new cases $m = 15, 42, 82, 123, 162, 243, 322, 366, 483, \dots$. The embedding of K_{15} also features in the following result, which shows that of the 12 residual classes that need to be resolved modulo 24, only 6 of these are actually required.

Proposition 5.10. *Suppose there exists an orientable hamilton cycle embedding of K_{15} and of K_n for all $n \geq 11$ such that $n \equiv 7, 11, 14, 19, 22$ or $23 \pmod{24}$. Then there exists an orientable hamilton cycle embedding of K_n for all $n \equiv 2$ or $3 \pmod{4}$, $n \notin \{2, 6, 7\}$.*

Proof. There is trivially no such embedding when $n = 2$, and Jungerman [9] showed that there are no orientable hamilton cycle embeddings of K_6 or K_7 . We show how to cover the remaining residual classes, proceeding by induction on n . The graph K_3 has an obvious hamilton cycle embedding in the sphere, and we know the required embedding exists for K_{10} from Theorem 5.5, so the proposition holds for $n \leq 10$.

Assume the proposition holds for all $n' < n$, where $n \equiv 2$ or $3 \pmod{4}$ and $n \geq 11$. If $n \equiv 7, 11, 14, 19, 22$ or $23 \pmod{24}$, then an orientable hamilton cycle embedding of K_n exists by assumption. If $n \equiv 2, 3, 6, 10, 15$ or $18 \pmod{24}$, then either $n \equiv 2 \pmod{8}$, or $n \equiv 3$ or $6 \pmod{12}$.

Suppose first that $n \equiv 2 \pmod{8}$, so $n \geq 18$. Then $n = 8p + 2 = 2(4p + 2) - 2$, where $4p + 2 \geq 10$. By induction K_{4p+2} has the required embedding, so by Theorem 5.3 K_n has the required embedding as well.

Suppose now that $n \equiv 3 \pmod{12}$. The required embedding exists for $n = 15$ by assumption, so we may suppose that $n \geq 27$. Then $n = 12p + 3 = 3(4p + 2) - 3$, where $4p + 2 \geq 10$. By induction K_{4p+2} has the required embedding, so by Theorem 5.4 K_n has the required embedding as well.

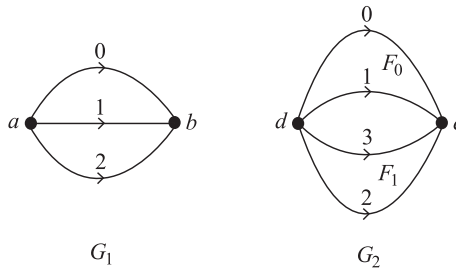
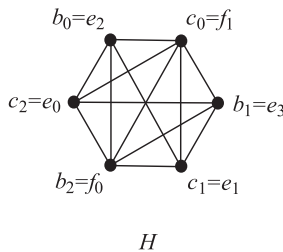
Finally, suppose that $n \equiv 6 \pmod{12}$. Since $n = 18$ is covered by the case of $n \equiv 2 \pmod{8}$, we may assume that $n \geq 30$. Then $n = 12p + 6 = 3(4p + 3) - 3$, where $4p + 3 \geq 11$. By induction K_{4p+3} has the required embedding, so by Theorem 5.4 K_n has the required embedding as well, and the proof is complete. ■

6. GENUS OF SOME COMPLETE QUADRIPARTITE GRAPHS

We use Lemma 5.1 to prove the following theorem.

Theorem 6.1. *For all $n \neq 2$, $g(K_{2n,n,n,n}) = g(K_{2n,3n}) = \lceil \frac{(n-1)(3n-2)}{2} \rceil$.*

Proof. We know from [18] that $g(K_{2n,3n}) = \lceil \frac{(n-1)(3n-2)}{2} \rceil$. Since $K_{2n,3n} \subset K_{2n,n,n,n}$, we have $g(K_{2n,n,n,n}) \geq \lceil \frac{(n-1)(3n-2)}{2} \rceil$. From Euler's formula, an embedding that achieves this genus must be a triangulation, so it will suffice to find an orientable triangulation of $K_{2n,n,n,n}$. By Theorem 4.2 there exists an orientable hamilton cycle embedding of $K_{n,n,n,n}$, and the desired triangulation follows from Lemma 5.1. ■

FIGURE 3. Embedded voltage graphs for derived embeddings Ψ_1 and Ψ_3 .FIGURE 4. Graph H that arises from diamond sum operation.

We would like to extend this theorem using the diamond sum technique. Before we can do that, however, we must address the case when $n = 2$. Because there is no orientable hamilton cycle embedding of $K_{2,2,2}$, no orientable triangulation of $K_{4,2,2,2}$ exists either; thus, contrary to expectations, $g(K_{4,2,2,2}) > \lceil \frac{(2-1)(6-2)}{2} \rceil = 2$. To provide a starting point for the diamond sum operation, we need to show that $g(K_{5,2,2,2}) = \lceil \frac{(5-2)(6-2)}{4} \rceil = 3$.

Let $\Psi_1 : K_{3,3} \hookrightarrow S_1$ be the embedding of $K_{3,3}$ that is derived from the embedded voltage graph G_1 with voltage group \mathbb{Z}_3 that is shown in Figure 3; this has three hamilton cycle faces C_0 , C_1 and C_2 . By placing a new vertex c_i in the center of each hamilton cycle face C_i and placing an edge between c_i and each vertex in C_i in the natural way, for $i \in \{0, 1, 2\}$, we obtain a triangulation $\Psi_2 : K_{3,3,3} \hookrightarrow S_1$. We can assume without loss of generality that the rotation graph around a_0 is given by the cycle $(b_0c_0b_1c_1b_2c_2)$.

Now let $\Psi_3 : K_{4,4} \hookrightarrow S_2$ be the embedding of $K_{4,4}$ that is derived from the embedded voltage graph G_2 with voltage group \mathbb{Z}_4 that is shown in Figure 3; this has two hamilton cycle faces F'_0 and F'_1 (derived from F_0 and F_1 in Figure 3, respectively) and four 4-cycle faces. By placing a new vertex f_i in the center of each hamilton cycle face F'_i and placing an edge between f_i and each vertex in F'_i in the natural way, for $i \in \{0, 1\}$, we obtain an embedding $\Psi_4 : K_{4,4,2} \hookrightarrow S_2$. The rotation graph around d_0 is given by the cycle $(e_0f_0e_1e_3f_1e_2)$.

We now form the diamond sum of Ψ_2 and Ψ_4 by removing the vertex a_0 and its neighborhood from Ψ_2 , removing the vertex d_0 and its neighborhood from Ψ_4 , and identifying the vertices around the boundaries of the holes as shown in Figure 4. Doing so yields an embedding $\overline{K_5} + H \hookrightarrow S_3$, where $V(\overline{K_5}) = \{a_1, a_2, d_1, d_2, d_3\}$ and H is the graph shown in Figure 4. Note that $H \cong K_{2,2,1,1}$; thus, we have an embedding of $K_{5,2,2,1,1}$ in the orientable surface S_3 . Since $K_{5,6} \subset K_{5,2,2,2} \subset K_{5,2,2,1,1}$, we know $3 = g(K_{5,6}) \leq g(K_{5,2,2,2}) \leq 3$, as required.

We are now able to extend Theorem 6.1 using the application of the diamond sum technique alluded to in Section 2.

Corollary 6.2. *For all $n \geq 1$ and all $t \geq 2n$, except $(n, t) = (2, 4)$, $g(K_{t,n,n}) = g(K_{t,3n}) = \lceil \frac{(t-2)(3n-2)}{4} \rceil$. Also, $g(K_{4,2,2,2}) = 3$.*

Proof. We know that $K_{t,3n} \subseteq K_{t,n,n,n}$, and from [18] we know $g(K_{t,3n}) = \lceil \frac{(t-2)(3n-2)}{4} \rceil$, so $g(K_{t,n,n,n}) \geq \lceil \frac{(t-2)(3n-2)}{4} \rceil$. If $n \neq 2$, we apply the diamond sum construction to orientable minimum genus embeddings of $K_{2n,n,n,n}$ and $K_{t-2n+2,3n}$. By Theorem 6.1 we know $g(K_{2n,n,n,n}) = \lceil \frac{(n-1)(3n-2)}{2} \rceil = \frac{(n-1)(3n-2)}{2}$, and again by [18] we know $g(K_{t-2n+2,3n}) = \lceil \frac{(t-2n)(3n-2)}{4} \rceil$. Via the diamond sum construction, we learn that $g(K_{t,n,n,n}) \leq \frac{(n-1)(3n-2)}{2} + \lceil \frac{(t-2n)(3n-2)}{4} \rceil = \lceil \frac{(t-2)(3n-2)}{4} \rceil$, and the result follows. If $n = 2$, we apply the diamond sum construction to orientable minimum genus embeddings of $K_{5,2,2,2}$ and $K_{t-3,6}$. As mentioned before, $g(K_{4,2,2,2}) > 2$; because $K_{4,2,2,2} \subset K_{5,2,2,2}$, we know $g(K_{4,2,2,2}) \leq g(K_{5,2,2,2}) = 3$ as well, so $g(K_{4,2,2,2}) = 3$. ■

Remark 6.3. We can use the above results to determine the genus of some large families of graphs. Corollary 6.2 implies that for all $n \geq 1$ and all $t \geq 2n$, except $(n, t) = (2, 4)$, and for any graph G satisfying $\overline{K_{3n}} \subseteq G \subseteq K_{n,n,n}$, the genus of $\overline{K_t} + G$ is the same as the genus of $K_{t,3n}$. In other words, $g(\overline{K_t} + G) = \lceil \frac{(t-2)(3n-2)}{4} \rceil$. If $n = 2$ and $\overline{K_6} \subseteq G \subseteq K_{2,2,2}$, then $g(\overline{K_4} + G) \in \{2, 3\}$. Moreover, in the special case $t = 2n$ and $n \neq 2$, we also get $g(G + H) = \lceil \frac{(n-1)(3n-2)}{2} \rceil$ for graphs G and H satisfying $\overline{K_{3n}} \subseteq G \subseteq K_{2n,n}$ and $\overline{K_{2n}} \subseteq H \subseteq K_{n,n}$.

Remark 6.4. If $n, t \geq 1$ and $t < 2n$, then we have $g(K_{t,n,n,n}) \geq g(K_{t+n,2n}) = \lceil \frac{(t+n-2)(2n-2)}{4} \rceil > \max(0, \lceil \frac{(t-2)(3n-2)}{4} \rceil) = g(K_{t,3n})$, except when $(n, t) = (1, 1)$ or $(3, 5)$. Thus, the genus formula from Corollary 6.2 generally does not hold for $t < 2n$. For $(n, t) = (1, 1)$ the formula does hold ($K_{1,1,1,1} = K_4$, which is planar). For $(n, t) = (3, 5)$ we do not know if $g(K_{5,3,3,3})$ is equal to $g(K_{8,6}) = g(K_{5,9}) = 6$.

ACKNOWLEDGMENTS

We thank both referees for helpful comments, and Terry Griggs for informing us of Širáň's embedding of K_{15} , mentioned in Section 5.

REFERENCES

- [1] A. Bouchet, Orientable and nonorientable genus of the complete bipartite graph, *J Combin Theory Ser B* 24 (1978), 24–33.
- [2] D. L. Craft, On the genus of joins and compositions of graphs, *Discrete Math* 178 (1998), 25–50.
- [3] M. N. Ellingham and J. Z. Schroeder, Nonorientable hamilton cycle embeddings of complete tripartite graphs, *Discrete Math* 312 (2012), 1911–1917.
- [4] M. N. Ellingham and Justin Z. Schroeder, Orientable hamilton cycle embeddings of complete tripartite graphs I: latin square constructions, *J Combin Des* 22 (2014), 71–94.

- [5] M. N. Ellingham and D. Christopher Stephens, The nonorientable genus of joins of complete graphs with large edgeless graphs, *J Combin Theory Ser B* 97 (2007), 827–845.
- [6] M. N. Ellingham and D. Christopher Stephens, The orientable genus of some joins of complete graphs with large edgeless graphs, *Discrete Math* 309 (2009), 1190–1198.
- [7] M. N. Ellingham, D. Christopher Stephens and X. Zha, The nonorientable genus of complete tripartite graphs, *J Combin Theory Ser B* 96 (2006), 529–559.
- [8] J. L. Gross and T. W. Tucker, *Topological Graph Theory*, Dover, Mineola, New York, 2001.
- [9] M. Jungerman, Orientable triangular embeddings of $K_{18} - K_3$ and $K_{13} - K_3$, *J Combin Theory Ser B* 16 (1974), 293–294.
- [10] M. Jungerman, The genus of the symmetric quadripartite graph, *J Combin Theory Ser B* 19 (1975), 181–187.
- [11] M. Jungerman, The nonorientable genus of the symmetric quadripartite graph, *J Combin Theory Ser B* 26 (1979), 154–158.
- [12] K. Kawarabayashi, D. Christopher Stephens and X. Zha, Orientable and nonorientable genera for some complete tripartite graphs, *SIAM J Discrete Math* 18 (2005), 479–487.
- [13] V. P. Korzhik, Triangular embeddings of $K_n - K_m$ with unboundedly large m , *Discrete Math* 190 (1998), 149–162.
- [14] Z. Magajna, B. Mohar and T. Pisanski, Minimal ordered triangulations of surfaces, *J Graph Theory* 10 (1986), 451–460.
- [15] T. A. McCourt, Biembedding a Steiner triple system with a hamilton cycle decomposition of a complete graph, *J Graph Theory*, to appear (available online November 27, 2013).
- [16] B. Mohar, T. D. Parsons and T. Pisanski, The genus of nearly complete bipartite graphs, *Ars Combin* 20B (1985), 173–183.
- [17] B. Mohar and C. Thomassen, *Graphs on Surfaces*, Johns Hopkins University Press, Baltimore, 2001.
- [18] G. Ringel, Das Geschlecht des vollständigen paaren Graphen, *Abh Math Sem Univ Hamburg* 28 (1965), 139–150.
- [19] A. T. White, *Graphs, Groups and Surfaces*, revised edition, North-Holland, Amsterdam, 1984.